COMPUTATIONAL METHODS IN APPLIED MATHEMATICS, Vol. 7 (2007), No. 3, pp. 264–282

FULLY AND SEMI-DISCRETE FOURTH-ORDER SCHEMES FOR HYPERBOLIC CONSERVATION LAWS

Y. H. ZAHRAN[1]

Abstract — A new fourth order accurate centered finite difference scheme for the solution of hyperbolic conservation laws is presented. A technique of making the fourth order scheme TVD is presented. The resulting scheme can avoid spurious oscillations and preserve fourth order accuracy in smooth parts. We discuss the extension of the TVD scheme to the nonlinear scalar hyperbolic conservation laws. For nonlinear systems, the TVD constraint is applied by solving shallow water equations. Then, we propose to use this fourth order flux as a building block in spatially fifth order weighted essentially non-oscillatory (WENO) schemes. The numerical solution is advanced in time by the third order TVD Runge — Kutta method. The performance of the scheme is assessed by solving test problems. The numerical results are presented and compared to the exact solutions and other methods.

2000 Mathematics Subject Classification: 65M12, 65M06, 35L65.

Keywords: conservation laws, difference schemes, TVD schemes, MUSCL schemes, WENO, shallow water equations.

1. Introduction

In recent years, a tremendous amount of research has been done in developing and implementing modern high-resolution methods for approximating solutions of hyperbolic conservation laws.

Among the variety of methods for approximating solutions of such problems we focus on finite difference methods, which can be divided into two main categories, namely upwind schemes and centered schemes.

The prototype of upwind schemes is the first order Godunov scheme in which a piecewise constant interpolated (which is constructed based on previously computed cell averages) is evolved exactly to the next time step according to the conservation laws. This evolution involves a solution of Riemann Problems (RP) on the boundaries of each cell, which is interpreted as an up-winding procedure, as one has to differentiate between the left-going and the right-going waves in order to compute the intercell flux in the nonsmooth regions.

An important issue is to how to generalize the first-order Godunov method to a second or higher order accuracy. Van Leer [12] proposed his monotone upwind schemes for the conservation laws (MUSCL) approach, whereby the piecewise constant cell average states in the Godunov method are replaced by reconstructed states that admit spatial variation within each cell. A class of second-order Godonuv-type (upwind) methods based on this approach have been constructed. Examples are MUSCL-Hancock schemes [12].

[1] *Physics and Mathematics Department Faculty of Engineering*, Port Said, Egypt. E-mail: yousef_hashem_zahran@yahoo.com

Centered (non-upwind or symmetric) schemes do not explicitly use the wave propagation information. The main advantage of centered over upwind schemes is that they do not require the solutions of Riemann problems or the computation of characteristic velocities of the system. These features make the centered schemes approach very attractive for these systems, for which the solution to the Riemann problem is complicated or when there is no simple analytical expression for the eigenvalues of the Jacobian matrix.

Godunov proved that monotone numerical schemes cannot be of accuracy greater than one. Much work has been done which involves the design of schemes that must necessarily be linear, even if applied to nonlinear problems. Among successful developments in this direction we have the TVD [4] and the WENO [6] and [2] methods. The main property of TVD schemes is that they avoid oscillations by locally reverting to the first order of accuracy near discontinuities and extrema which make them unsuitable for applications involving long time evolution of complex structures. For these applications we need uniformly very high order methods, e.g., WENO methods. The WENO idea is to obtain a self-similar (i. e., mesh size dependent parameter), uniformly high-order accurate, yet essentially non-oscillatory scheme (i. e., the magnitude of the oscillations decay as $o(\Delta x)^k$, where k is the order of accuracy) for piecewise smooth functions. The main advantage of the WENO scheme is it can be of $(2k-1)$-th order spatial accuracy in smooth regions and emulates the k-th order near discontinuities.

In this paper, we use the MUSCL-Hancock (upwind) approach to construct, for the linear case, a fourth order centered scheme, in which the Godunov first-order upwind scheme is replaced by the second order centered scheme presented in [15], thus eliminating the need for the RP altogether. A TVD version of this scheme is then constructed; this requires the formulation of TVD conditions that are suitable for the scheme. We also present ways of extending the scheme to the nonlinear scalar case. Some numerical results are also presented. The extension of the third order to nonlinear hyperbolic conservation laws is validated by solving a test problem for shallow water equations.

Titarev and Toro [14] proposed to use second order TVD fluxes as a building block in high-order methods and applied the principle to the WENO scheme. They used fifth-order WENO reconstruction and a second order TVD flux. They showed, from the numerical results, that their new methods are superior to the original schemes using first order fluxes. In this paper, we propose to use the fourth order flux, presented here, instead of the Toro second order TVD flux, as a building block in spatially fifth order WENO reconstruction. The use of this flux within the WENO framework improves the order of accuracy, convergence and better resolution of discontinuities. Compared to the Toro scheme, the new flux improves upon Toro flux in terms of the order of accuracy, convergence and better resolution of discontinuities.

The paper is organized as follows: in section 2, we briefly review the general framework of upwind and centered schemes. In section 3 we construct the fourth order accurate centered scheme following the MUSCL-Hancock approach. In section 4, we develop a TVD version of the scheme. In section 5, we extend the previous scheme to nonlinear scalar problems. In section 6 , we extend the scheme to constant coefficients linear hyperbolic conservation laws. Section 7 discusses nonlinear systems typically the shallow water equations. In section 8, we briefly review the WENO reconstruction and the TVD Runge — Kutta method for time discretization. Also, we present the WENO-TVD method.

Numerical tests on the linear equations with different initial conditions, nonlinear Burger equations and shallow water equations are performed in section 9. The numerical results are presented and compared to the exact solutions. The efficiency of the scheme is shown numerically by comparison with other schemes. The conclusion is presented in section 10.

2. Review of the difference schemes

Consider the hyperbolic conservation law

$$U_t + F(U)_x = 0, \quad -\infty < x < \infty, \quad t \geqslant 0 \tag{2.1}$$

along with the initial and boundary conditions. Where U is the vector of m unknown conservative variables and F(U) is the corresponding vector of fluxes. Consider now a control volume in $x - t$ space $I_j \times [t^n, t^{n+1}]$ of dimension. $\Delta x = x_{j+1/2} - x_{j-1/2}$, $\Delta t = t^{n+1} - t^n$, where $I_j = [x_{j-1/2}, x_{j+1/2}]$. Integrating (2.1) on this control volume produce the conservative formula

$$U_j^{n+1} = U_j^n - \lambda[F_{j+1/2}^n - F_{j-1/2}^n], \quad \lambda = \frac{\Delta t}{\Delta x} \tag{2.2}$$

where U_j^n, $F_{j+1/2}^n$ are given by

$$U_j^n = \frac{1}{\Delta x} \int_{x_{j-1/2}}^{x_{j+1/2}} U(x, t^n)\, dx \quad \text{and} \quad F_{j+1/2}^n = \frac{1}{\Delta t} \int_{t^n}^{t^{n+1}} F(U(x_{j+1/2}, t)\, dt. \tag{2.3}$$

We can construct numerical methods based on the control volume (2.2) by finding numerical fluxes that are approximations to the time integral average of the fluxes at the control volume boundaries given in (2.3). The numerical scheme will then evolve in time integral averages in the control volumes. Next we briefly review the two classical ways of finding a numerical flux.

2.1. Upwind difference schemes. A prototype of such upwind schemes is the Godunov scheme . Godunov advanced the idea of computing the numerical flux in (2.2) by evaluating (2.3) in terms of the solution $U^*(x/t)$ of a local initial value problem called the Riemann problem (RP)

$$U_t + F(U)_x = 0, \quad U(x, 0) = \begin{cases} U_j^n, & x < x_{j+1/2}, \\ U_{j+1}^n, & x > x_{j+1/2}, \end{cases} \tag{2.4}$$

evaluated at the cell interface $x_{j+1/2}$.

Conventionally, the initial data $U(x, 0)$ in the RP represent a piecewise constant and consist of two constant states of the form (2.3) separated by a discontinuity. Such a distribution of the initial data is traditionally associated with a first order accurate Godunov type scheme with the numerical flux

$$F_{j+1/2} = F(U^*(0)) \tag{2.5}$$

obtained by evaluating the flux (2.3) with the integrand $F(U^*(x/t))$.

Van Leer [12] advanced the idea of modifying the piecewise constant data in the Godunov first order upwind method, as a way to achieve a higher order of accuracy. This approach has become known as the MUSCL scheme and has been used to construct high order upwind schemes. The first step common to all MUSCL schemes is the data reconstruction procedure.

2.1.1. Data reconstruction. The simplest way of modifying the piecewise constant data $\{U_j^n\}$ is to replace the U_j^n, understood as integral averages in the cells I_j, by piecewise linear functions $U_j(x)$, namely [11]

$$U_j(x) = U_j^n + \frac{(x - x_j)}{\Delta x}\Delta_j, \quad x \in [0, \Delta x], \tag{2.6}$$

where Δ_j is a suitably chosen slope of $U_j(x)$ in the cell I_j. The center of the cell x_j in the local coordinates is $x = \Delta x/2$ and $U_j(x_j) = U_j^n$. The boundary extrapolated values are

$$U_j^L(x) = U_j(0) = U_j^n - \frac{1}{2}\Delta_j, \quad U_j^R(x) = U_j(\Delta x) = U_j^n + \frac{1}{2}\Delta_j. \tag{2.7}$$

A possible choice of the slope Δ_j in (2.6) is

$$\Delta_j = \frac{1}{2}(1+\omega)\Delta_{j-1/2}U + \frac{1}{2}(1-\omega)\Delta_{j+1/2}U, \tag{2.8}$$

where ω is a free parameter in the real interval $[-1, 1]$. For $\omega = 0$, Δ_j is the central difference approximation to the first spatial derivative. Here $\Delta_{j+1/2}u = u_{j+1} - u_j$.

2.1.2. MUSCL-Hancock approach. Having modified the data, we have several ways of using the Godunov first order upwind method to obtain high order schemes. One possible choice is the MUSCL-Hancock approach [13]. This has three steps, namely [10]:

i) Data reconstruction as in (2.6) with boundary extrapolated values as in (2.7).

ii) Evolution of $\bar{U}_j^L$, $\bar{U}_j^R$ by a time $\Delta t/2$ according to

$$\bar{U}_j^L = U_j^L + \frac{1}{2}\lambda[F(U_j^L) - F(U_j^R)], \quad \bar{U}_j^R = U_j^R + \frac{1}{2}\lambda[F(U_j^L) - F(U_j^R)]. \tag{2.9}$$

iii) Solution of the piecewise constant data RP for the appropriate conservation laws with the initial data $\bar{U}_j^R$, $\bar{U}_{j+1}^L$ to find the similarity solution $U_{j+1/2}(x/t)$.

In the conventional MUSCL-Hancock scheme, the inter-cell numerical flux $F_{j+1/2}$ is then obtained in exactly the same way as in the Godunov first order upwind method, namely $F_{j+1/2} = F(U^*_{j+1/2}(0))$.

2.2. Centered schemes. Centered (non-upwind or symmetric) schemes do not explicitly utilize the wave propagation of information and are thus simpler and more generally applicable. Commonly, the numerical fluxes can be computed explicitly as algebraic functions of the initial condition in (2.4), namely

$$F_{j+1/2} = F_{j+1}(U^n_{j+1/2}, U^n_{j+1}), \tag{2.10}$$

for example, first order Lax — Friedrichs (LxF) and second order Lax — Wendroff (L-W). In [15], a second order centered scheme was presented.

For the scalar hyperbolic conservation law, namely

$$u_t + f(u)_x = 0. \tag{2.11}$$

Here u is the unknown function and $f(u)$ is the physical flux. First let us consider the linear case where $f(u) = au$ so that $f'(u) = a$ is a constant wave velocity speed.

The conservative numerical scheme introduced in [15] has the form

$$u_j^{n+1} = u_j^n - \lambda[F^n_{j+1/2} - F^n_{j-1/2}] \tag{2.12.a}$$

with the numerical flux

$$F_{j+1/2} = \frac{1}{2}(au_j + au_{j+1}) - \frac{1}{2}|a|\Delta_{j+1/2}u + |a|\{A_0\Delta_{j+1/2}u + A_1\Delta_{j+L+1/2}u + A_2\Delta_{j+M+1/2}u\}, \tag{2.12.b}$$

where

$$A_0 = \frac{1}{2} - \frac{|c|}{4}, \quad A_1 = -\frac{1}{8} - \frac{|c|}{8}, \quad A_2 = \frac{1}{8} - \frac{|c|}{8}, \tag{2.12c}$$

$L = -1$, $M = 1$ for $c > 0$ and $L = 1$, $M = -1$ for $c < 0$. Here $c = a\Delta t/\Delta x$ is the Courant number.

The above flux includes a five point second order scheme. The scheme is stable for $|c| \leqslant \sqrt{2}$.

In the next section we use the MUSCL-Hancock approach to construct a centered scheme, in which the Godonuv first order upwind method is replaced by the second order centered scheme (2.12), thus eliminating the need of the RP altogether.

3. Centered MUSCL-Hancock method

Here we modify the MUSCL-Hancock scheme, mentioned in the previous section, by replacing the Godunov first order upwind method in step III by the second order centered scheme (2.12). In this way , the role of the RP is eliminated altogether. Now, instead of solving the RP with the data $(\bar{U}_j^R, \bar{U}_{j+1}^L)$ to find the Godunov first order upwind flux, we evaluate the centered flux $F_{j+1/2}^C$. For the linear equation (2.11), the case of $F_{j+1/2}^C$ is given by (2.12b) and thus we have

$$F_{j+1/2}^C = \frac{1}{2}a(\bar{u}_j^R + \bar{u}_{j+1}^L) - \frac{1}{2}|a|(\bar{u}_{j+1}^L - \bar{u}_j^R) +$$

$$|a|\{A_0(\bar{u}_{j+1}^L - \bar{u}_j^R) + A_1(\bar{u}_j^L - \bar{u}_{j-1}^R) + A_2(\bar{u}_{j+2}^L - \bar{u}_{j+1}^R)\}, \tag{3.1}$$

where $\bar{U}_j^R$, $\bar{U}_j^L$ are given by (2.9). Direct substitution of this flux into the conservative formula (12a) gives a seven-point centered MUSCL-Hancock scheme, namely

$$u_j^{n+1} = \sum_{-3}^{3} b_k u_{j+k}^n \tag{3.2}$$

with coefficients

$$b_{-3} = \frac{1}{192}\{-6c + 6c^3 + 6c\omega - 6c^3\omega\}, \quad b_{-2} = \frac{1}{192}\{28c + 24c^2 - 12c^3 - 12c\omega - 12c^3\omega\},$$

$$b_{-1} = \frac{1}{192}\{18c + 14c^3 + 102c\omega - 6c^3\omega\}, \quad b_0 = \frac{1}{192}\{192 + 120c - 48c^{2-} 24c^3 - 180c\omega + 36c^3\omega\},$$

$$b_1 = \frac{1}{192}\{-178c + 18c^3 + 102c\omega - 6c^3\omega\}, \quad b_2 = \frac{1}{192}\{12c + 24c^2 + 4c^3 - 12c\omega - 12c^3\omega\},$$

$$b_3 = \frac{1}{192}\{6c - 6c^3 - 6c\omega + 6c^3\omega\}. \tag{3.3}$$

Theorem 3.1. *Scheme* (3.2), (3.3) *is third order accurate in space and time for any value of* ω *and fourth order accurate in space and time when*

$$\omega = \frac{64c^3 - 32c^2 - 256c + 157}{384 - 192c^2}. \tag{3.4}$$

Proof. It can be shown [6] that a scheme for the linear equation (11) of the form (3.2) is pth order accurate in space and time if and only if

$$\sum k^q b_k = (-c)^q, \quad 0 \leqslant q \leqslant p. \tag{3.5}$$

The application of condition (3.5) to the scheme (3.2), (3.3) YIELDS the desired result. □

It is well known that the difference schemes that are second (or higher) order accurate produce spurious oscillations behind the waves and near discontinuities. This problem has frustrated researchers for many years until the concept and theory of TVD schemes were advanced by Harten [4]. The main property of the TVD scheme is that it can be second (or higher) order accurate and free of oscillations. A TVD version of this center scheme will be constructed in the next section.

4. TVD analysis for the fourth order scheme

Here we propose TVD criteria that are suitable for constructing TVD schemes based on the centered fourth order scheme (3.2)–(3.4). To this end we consider the model hyperbolic conservation law

$$u_t + f(u)_x = 0, \quad f(u) = au, \tag{4.1}$$

where a is constant.

The fourth order finite difference centered scheme constructed in the previous section can be written in the conservative form as

$$u_j^{n+1} = u_j^n - \lambda[F_{j+1/2}^n - F_{j-1/2}^n] \tag{4.2}$$

with the numerical flux

$$F_{j+1/2} = \frac{1}{2}(f_j + f_{j+1}) - \frac{1}{2}|a|\Delta_{j+1/2}u +$$

$$|a|\{A_0\Delta_{j+1/2}u + A_1\Delta_{j+L+1/2}u + A_2\Delta_{j+M+1/2}\} + |a|\{A_3\Delta_{j+S+1/2} + A_4\Delta_{j+Q+1/2}u\} \tag{4.3}$$

where

$$A_0 = \frac{1}{192}\{59 + 96\omega + 48c + 8c^2 - 48c^2\omega\}, \quad A_1 = \frac{1}{192}\{176 + 24c - 36\omega + 12c^2\omega\},$$

$$A_2 = \frac{1}{192}\{24 + 24c - 8c^2 - 24c\omega\}, \quad A_3 = \frac{1}{192}\{-6 + 6c^2 + 6\omega - 6c^2\omega\},$$

$$A_4 = \frac{1}{192}\{6 - 6c^2 - 6\omega + 6c^2\omega\} \tag{4.4}$$

$L = -1$, $M = 1$, $S = -2$, $Q = 2$ for $c > 0$ and $L = 1$, $M = -1$, $S = 2$, $Q = -2$ for $c < 0$.

We assume that scheme (4.2) can be expressed as

$$u_j^{n+1} = u_j^n - B_{j-1/2}\Delta_{j-1/2}u + C_{j+1/2}\Delta_{j+1/2}u, \tag{4.5a}$$

where $B_{j+1/2}$ and $C_{j+1/2}$ are data-dependent coefficients, i. e., functions of the set $\{u_j^n\}$.

To apply the TVD concept, we use Harten's theorem [4], which states that: the scheme (4.5a) is TVD provided that

$$B_{j+1/2} \geqslant 0, \quad C_{j+1/2} \geqslant 0, \quad B_{j+1/2} + C_{j+1/2} \leqslant 1. \tag{4.5b}$$

Imposing a TVD constraint on (4.3) via flux limiter functions gives

$$F_{j+1/2} = \frac{1}{2}(f_j + f_{j+1}) - \frac{1}{2}|a|\Delta_{j+1/2}u + |a|\{A_0\Delta_{j+1/2}u + A_1\Delta_{j+L+1/2}u\}\phi_j +$$

$$|a|\{A_2\Delta_{j+M+1/2}u + A_3\Delta_{j+S+1/2} + A_4\Delta_{j+Q+1/2}u\}\phi_{j+M}, \tag{4.6}$$

where ϕ_j and ϕ_{j+M} are flux limiter functions.

Theorem 4.1. *Scheme* (4.2), (4.6) *is TVD for* $|c| \leqslant 1$ *if the limiter function is defined by*

$$\phi_j \leqslant \frac{(1-|c|)r_j}{\eta(A_1r_j + A_0 - A_2 - A_3r^*_{j-2}r_j + A_4r_j/r^{**}_j)}, \tag{4.7}$$

$$\phi_j \leqslant \frac{(1-|c|) + \eta(A_2/r^*_{j+1} + A_3r_j + A_4/r^{**}_{j+1})}{\eta(A_1r_j + A_0)}, \tag{4.8}$$

$$\phi_j \geqslant \frac{(A_2/r^*_{j+1} + A_3r_j + A_4/r^{**}_{j+1})}{(A_1r_j + A_0)}, \tag{4.9}$$

$$\phi_j \geqslant 0, \tag{4.10}$$

where

$$r_j = \frac{\Delta_{j+L+1/2}u}{\Delta_{j+1/2}u}, \quad r^*_j = \frac{\Delta_{j+L+1/2}u}{\Delta_{j+M+1/2}u}, \quad r^{**}_j = \frac{\Delta_{j+L+1/2}u}{\Delta_{j+Q+1/2}u}, \tag{4.11}$$

and η *is defined by*

$$\eta = \begin{cases} 1-|c|, & \text{for } 0 \leqslant |c| < 1/2, \\ |c|, & \text{for } 1/2 \leqslant |c| \leqslant 1. \end{cases} \tag{4.12}$$

Proof. Firstly, consider the method with Courant $0 \leqslant c \leqslant 1$. From (4.2) and (4.6) the numerical method is

$$u^{n+1}_j = u^n_j - c[\Delta_{j-1/2}u^n + A_0\Delta_{j+1/2}u^n\phi_j + A_1\Delta_{j-1/2}u^n\phi_j - A_0\Delta_{j-1/2}u^n\phi_{j-1} - A_1\Delta_{j-}u^n\phi_{j-1}] -$$

$$c[A_2\Delta_{j+1/2}u^n\phi_{j+1} + A_3\Delta_{j-1/2}u^n\phi_{j+1} + A_4\Delta_{j+1/2}u^n\phi_{j+1}] +$$

$$c[A_2\Delta_{j+1/2}u^n\phi_j + A_3\Delta_{j-1/2}u^n\phi_j + A_4\Delta_{j+1/2}u^n\phi_j]. \tag{4.13}$$

This is equivalent to Harten's theorem (4.5), with the choice of

$$B_{j-1/2} = c\left[1 + \frac{A_0}{r_j}\phi_j + A_1\phi_j - A_0\phi_{j-1} - A_1r_{j-1}\phi_{j-1}\right] +$$

$$c\left[\frac{A_2}{r^*_j}\phi_{j+1} + A_3r_{j-1}\phi_{j+1} + \frac{A_4}{r^{**}_j}\phi_{j+1}\right] + c\left[-\frac{A_2}{r_j}\phi_j - A_3r^*_{j-2}\phi_j - \frac{A_4}{r^{**}_j}\phi_j\right], \tag{4.14}$$

$$C_{j+1/2} = 0, \tag{4.15}$$

we apply condition (4.5) to (4.14), i. e.,

$$0 \leqslant c\left[1 + \frac{A_0}{r_j}\phi_j + A_1\phi_j - A_0\phi_{j-1} - A_1r_{j-1}\phi_{j-1}\right] + c\left[\frac{A_2}{r^*_j}\phi_{j+1} + A_3r_{j-1}\phi_{j+1} + \frac{A_4}{r^{**}_j}\phi_{j+1}\right] +$$

$$c\left[-\frac{A_2}{r_j}\phi_j - A_3r^*_{j-2}\phi_j - \frac{A_4}{r^{**}_j}\phi_j\right] \leqslant 1, \tag{4.16}$$

one way to satisfy these inequalities is by imposing

$$\left[\frac{A_0}{r_j}+A_1-\frac{A_2}{r_j}-A_3r^*_{j-2}-\frac{A_4}{r^{**}_j}\right]\phi_j-\left[A_0+A_1r_{j-1}\right]\phi_{j-1}+\left[\frac{A_2}{r^*_j}+A_3r_{j-1}+\frac{A_4}{r^{**}_j}\right]\phi_{j+1}\leqslant\frac{1-c}{c},\tag{4.17}$$

$$\left[A_0+A_1r_{j-1}\right]\phi_{j-1}-\left[\frac{A_2}{r^*_j}+A_3r_{j-1}+\frac{A_4}{r^{**}_j}\right]\phi_{j+1}-\left[\frac{A_0}{r_j}+A_1-\frac{A_2}{r_j}-A_3r^*_{j-2}-\frac{A_4}{r^{**}_j}\right]\phi_j\leqslant 1,\tag{4.18}$$

from (4.17) we have

$$0\leqslant\left[\frac{A_0}{r_j}+A_1-\frac{A_2}{r_j}-A_3r^*_{j-2}-\frac{A_4}{r^{**}_j}\right]\phi_j\leqslant\frac{1-c}{c},\tag{4.19}$$

$$0\leqslant\left[A_0+A_1r_{j-1}\right]\phi_{j-1}-\left[\frac{A_2}{r^*_j}+A_3r_{j-1}+\frac{A_4}{r^{**}_j}\right]\phi_{j+1}\leqslant\frac{1-c}{c},\tag{4.20}$$

and from (4.18) we get

$$0\leqslant\left[A_0+A_1r_{j-1}\right]\phi_{j-1}-\left[\frac{A_2}{r^*_j}+A_3r_{j-1}+\frac{A_4}{r^{**}_j}\right]\phi_{j+1}\leqslant 1,\tag{4.21}$$

$$0\leqslant\left[\frac{A_0}{r_j}+A_1-\frac{A_2}{r_j}-A_3r^*_{j-2}-\frac{A_4}{r^{**}_j}\right]\phi_j\leqslant 1,\tag{4.22}$$

from (4.19) we get

$$\phi_j\leqslant\frac{(1-c)r_j}{c\left(A_0+A_1r_j-A_2-A_3r_jr^*_{j-2}+A_4r_j/r^{**}_j\right)},\tag{4.23}$$

and from (4.22) we get

$$\phi_j\leqslant\frac{r_j}{c\left(A_0+A_1r_j-A_2-A_3r_jr^*_{j-2}+A_4r_j/r^{**}_j\right)},\tag{4.24}$$

from (4.20) and (4.21) we obtain

$$\phi_j\leqslant\frac{1-c+c\left[A_2/r^*_{j+1}+A_3r_j+A_4/r^{**}_{j+1}\right]}{c\left(A_0+A_1r_j\right)}\phi_{j+2},\tag{4.25}$$

$$\phi_j\leqslant\frac{1+\left[A_2/r^*_{j+1}+A_3r_j+A_4/r^{**}_{j+1}\right]}{\left(A_0+A_1r_j\right)}\phi_{j+2},\tag{4.26}$$

and

$$\phi_j\geqslant\frac{A_2/r^*_{j+1}+A_3r_j+A_4/r^{**}_{j+1}}{\left(A_0+A_1r_j\right)}\phi_{j+2},\tag{4.27}$$

$$\phi_j\geqslant 0,\tag{4.28}$$

then from (4.23) and (4.24) we have

$$\phi_j\leqslant\frac{(1-|c|)r_j}{\eta(A_1r_j+A_0-A_2-A_3r^*_{j-2}r_j+A_4r_j/r^{**}_j)},\tag{4.29}$$

$$\phi_j \leqslant \frac{(1-|c|)+\eta(A_2/r^*_{j+1}+A_3r_j+A_4/r^{**}_{j+1})}{\eta(A_1r_j+A_0)}\phi_{j+2}, \tag{4.30}$$

$$\phi_j \geqslant \frac{A_2/r^*_{j+1}+A_3r_j+A_4/r^{**}_{j+1}}{A_1r_j+A_0}\phi_{j+2}, \tag{4.31}$$

where η is defined by equation (4.12). The analysis for $-1 \leqslant c \leqslant 0$ goes through an exactly the same way, but c is replaced by $|c|$ and ϕ_{j+2} is replaced by ϕ_{j-2} . Finally, by setting $\phi_{j+2} = 1$ or $\phi_{j-2} = 1$ the theorem is proved [7].

By applying the last theorem to scheme (4.2), (4.6), the flux limiter can be defined as

$$\phi_j = \begin{cases} \dfrac{(1-|c|)r_j}{\eta(A_1r_j+A_0-A_2-A_3r^*_{j-2}r_j+A_4r_j/r^{**}_j)}, & 0 \leqslant r_j \leqslant r^L, \\ 1, & r^L \leqslant r_j \leqslant r^R, \\ \dfrac{(1-|c|)+\eta(A_2/r^*_{j+1}+A_3r_jr_j+A_4/r^{**}_{j+1})}{\eta(A_1r_j+A_0)}, & r_j \geqslant r^R, \\ 0, & r_j \leqslant 0. \end{cases} \tag{4.32}$$

5. Extension to nonlinear scalar hyperbolic conservation laws

To extend scheme (4.2), (4.6) to nonlinear scalar problems, we consider the equation

$$u_t + f(u)_x = 0. \tag{5.1}$$

Define the wave velocity

$$a_{j+1/2} = \begin{cases} \Delta_{j+1/2}f/\Delta_{j+1/2}u, & u/\Delta_{j+1/2}u \neq 0, \\ \partial f/\partial u|_{u_j}, & \Delta_{j+1/2}u = 0. \end{cases} \tag{5.2}$$

Now we redefine the r_j in (4.11) as

$$r_j = \frac{|a_{j+L+1/2}|\Delta_{j+L+1/2}u}{|a_{j+1/2}|\Delta_{j+1/2}u}, \quad r^*_j = \frac{|a_{j+L+1/2}|\Delta_{j+L+1/2}u}{|a_{j+M+1/2}|\Delta_{j+M+1/2}u}, \quad r^{**}_j = \frac{|a_{j+L+1/2}|\Delta_{j+L+1/2}u}{|a_{j+Q+1/2}|\Delta_{j+Q+1/2}u}. \tag{5.3}$$

Here $c_{j+1/2} = a_{j+1/2}\Delta t/\Delta x$.

Unlike the constant coefficient case, $a_{j+1/2}$ and $a_{j-1/2}$ are not always of the same sign. Then the numerical flux (4.6) takes the form

$$F_{j+1/2} = \frac{1}{2}(f_j+f_{j+1}) - \frac{1}{2}|a_{j+1/2}|\Delta_{j+1/2}u + |a_{j+1/2}|\{A_0\Delta_{j+1/2}u + A_1\Delta_{j+L+1/2}u\}\phi_j +$$

$$|a_{j+1/2}|\{A_2\Delta_{j+M+1/2}u + A_3\Delta_{j+S+1/2} + A_4\Delta_{j+Q+1/2}u\}\phi_{j+M}, \tag{5.4}$$

where

$$r^L = \frac{\eta(A_0-A_2-A_3r^*_{j-2})}{1-|c|-\eta\,A_1-\eta\,A_4/r^{**}_j}, \quad r^R = \frac{1-|c|-\eta\,(A_0-A_2/r^*_{j+1}-A_4/r^{**}_{j+1})}{\eta\,(A_1-A_3)}, \tag{4.33}$$

Therefore scheme (4.2), (4.6) becomes TVD. After considering all the possible combinations of the signs of $a_{j+1/2}$ and $a_{j-1/2}$, a set of sufficient conditions on ϕ still can be of the form similar to (4.32) by replacing c by $a_{j+1/2}$.

6. Application to linear hyperbolic systems

In this section, we extend the scalar schemes (4.2), (4.6) to solve the initial value problem for linear hyperbolic systems with constant coefficients

$$U_t + AU_x = 0, \quad U(x,0) = U_0(x), \tag{6.1}$$

where U is a column vector of m conserved variables and A is an $m \times m$ constant matrix. This is a system of conservation laws with the flux function $F(U) = AU$ which is hyperbolic if A is diagonalizable with real eigenvalues, i. e., the matrix A can be written as

$$A = R\Omega R^{-1}, \tag{6.2}$$

where $\Omega = \operatorname{diag}(\lambda^{(1)}, \lambda^{(2)}, \ldots, \lambda^{(m)})$ is the diagonal matrix of the eigenvalues of A and $R = (r(1), r(2), \ldots, r(m))$ is the matrix of the right eigenvectors of A.

Equation (6.2) means $AR = R\Omega$, i. e.,

$$Ar^{(p)} = \lambda^{(p)} r^{(p)}, \quad p = 1, 2, \ldots, m. \tag{6.3}$$

A natural way to extend the scalar scheme to linear systems is obtained by defining the expressions for the flux differences $\Delta_{j+1/2}F = A\Delta_{j+1/2}U$.

This can be done by diagonalizing the system solving the local Riemann problems with the left and right states U_j^n and U_{j+1}^n, i. e.,

$$U(x,0) = \begin{cases} U_j^n, & x < 0, \\ U_{j+1}^n, & x > 0, \end{cases} \tag{6.4}$$

and letting

$$\alpha_{j+1/2} = R_{j+1/2}^{-1} \Delta_{j+1/2} U, \tag{6.5}$$

where $R_{j+1/2}$ is the matrix of the right eigenvectors at the interface $(j+1/2)$, which for the linear constant coefficient case is of course constant; $\alpha_{j+1/2}$ is called the wave strength vector with components $\alpha_{j+1/2}^{(p)}$, $(p = 1, 2, \ldots, m)$ across the p-the wave travelling at velocity $\lambda_{j+1/2}^{(p)}$ in the $(j+1/2)$ intercell. Then we have

$$\Delta_{j+1/2} U = \sum_{p=1}^{m} \alpha_{j+1/2}^{(p)} r_{j+1/2}^{(p)}. \tag{6.6}$$

Since $F(U) = AU$, this leads to

$$\Delta_{j+1/2} F = A\Delta_{j+1/2} U = \sum_{p=1}^{m} \alpha_{j+1/2}^{(p)} A r_{j+1/2}^{(p)} = \sum_{p=1}^{m} \alpha_{j+1/2}^{(p)} \lambda_{j+1/2}^{(p)} r_{j+1/2}^{(p)}. \tag{6.7}$$

Note that the single jump $\Delta_{j+q+1/2}F = |a_{j+q+1/2}|\Delta_{j+q+1/2}U$ in the scalar scheme (5.4) with the appropriate interpretation for $|a_{j+1/2}|$ is now substituted by a summation of jump (6.7), which gives a natural extension to linear systems with constant coefficients.

7. Nonlinear hyperbolic systems

Let the nonlinear system of equations

$$U_t + F(U)_x = 0, \tag{7.1}$$

where $F(U)$ is a vector flux such that $A(U) = \partial F/\partial U$, be the Jacobian matrix.

A possible strategy for solving systems of nonlinear equations is to linearize the nonlinear system of equations (7.1) locally at each cell interface by approximating the Jacobian matrix $A(U)$ and then implement the method of the previous section using the linearized system

$$U_t + \bar{A}U_x = 0. \tag{7.2}$$

where $\bar{A}$ is a linearized constant matrix depending only on the local data U_j^n and U_{j+1}^n, i. e., $\bar{A} = \bar{A}(U_j^n, U_{j+1}^n)$. A popular example of this approach is Roe?s approximation [7] . Roe?s matrix $\bar{A}(U_j^n, U_{j+1}^n)$ is assumed to satisfy the following properties:

i) $\bar{A}\Delta_{j+1/2}U = \Delta_{j+1/2}F$;

ii) $\bar{A}$ is diagonalizable with real eigenvalues;

iii) $A \to F'(\bar{U})$ smoothly as U_j^n, $U_{j+1}^n \to \bar{U}$.

Denoting the Roe eigenvalues, the eigenvectors, and the wave strengths as $\bar{\lambda}_{j+1/2}^{(p)}$, $\bar{r}_{j+1/2}^{(p)}$, $\bar{\alpha}_{j+1/2}^{(p)}$ $(p = 1, 2, \ldots, m)$ respectively, then applying the fourth order scheme of the previous section, we solve the original nonlinear systems in a straightforward manner.

7.1. Shallow water equations. The one- dimensional shallow water equation as a typical nonlinear system of conservation law represents the motion of a free surface flow in a channel and takes the form [9]

$$U_t + F(U)_x = 0, \tag{7.3a}$$

where

$$U = (S, Su)^\top, \quad F(U) = \left(Su, Su^2 + S^2\right)^\top, \tag{7.3b}$$

where S is the cross-section of the flow, u is the velocity. With the initial conditions

$$U(x, t_0) = \begin{cases} U_L, & x < x_0, \\ U_R, & x > x_0. \end{cases} \tag{7.3c}$$

Equations (7.3) can be written in the form

$$U_t + A(U)U_x = 0, \quad A(U) = \frac{\partial F}{\partial U}, \tag{7.4}$$

where $A(U)$ is the Jacobian matrix such that

$$A = \begin{pmatrix} 0 & 1 \\ 2S - u^2 & 2u \end{pmatrix}. \tag{7.5}$$

System (7.3)–(7.5) is hyperbolic with the eigenvalues

$$\lambda^{(1)} = u - C, \quad \lambda^{(2)} = u + C, \tag{7.6}$$

where $C = \sqrt{2S}$ denotes the sound speed. The corresponding right eigenvectors of the Jacobian A are found to be

$$r^{(1)} = (1, u - C)^\top, \quad r^{(2)} = (1, u + C)^\top. \tag{7.7}$$

7.2. Linearization of shallow water equations. The nonlinear system of equations (7.3) can be linearized as

$$U_t + \bar{A}U_x = 0, \tag{7.8}$$

where $\bar{A}$ is an approximate Jacobian matrix of A with eigenvalues $\bar{\lambda}^{(p)}$ and eigen vectors $\bar{r}^{(p)}$ such that

$$\bar{A}\Delta U = \Delta F. \tag{7.9}$$

The approximate matrix Jacobian $\bar{A}$ satisfying (7.9) can be written as

$$\bar{A}(U_j, U_{j+1}) = \begin{pmatrix} 0 & 1 \\ \bar{C}^2 - \bar{u}^2 & 2\bar{u} \end{pmatrix}. \tag{7.10a}$$

where $\bar{C}$ and $\bar{u}$ are given by

$$\bar{C} = \sqrt{S_j + S_{j+1}}, \tag{7.10b}$$

$$\bar{u} = \frac{u_{j+1}\sqrt{S_{j+1}} + u_j\sqrt{S_j}u_{j+1}}{\sqrt{S_{j+1}} + \sqrt{S_j}}. \tag{7.10c}$$

The eigenvalues and eigenvectors of the linearized matrix $\bar{A}$ are

$$\bar{\lambda}^{(1)} = \bar{u} - \bar{C}, \quad \bar{\lambda}^{(2)} = \bar{u} + \bar{C}, \quad \bar{r}^{(1)} = \left(1, \bar{u} - \bar{C}\right)^\top, \quad \bar{r}^{(2)} = \left(1, \bar{u} + \bar{C}\right)^\top. \tag{7.11}$$

The wave strengths are

$$\bar{\alpha}^1 = 0.5\,\Delta S + \frac{1}{2C}(\bar{u}\Delta S - \Delta S u), \quad \bar{\alpha}^2 = 0.5\,\Delta S - \frac{1}{2C}(\bar{u}\Delta S - \Delta S u), \tag{7.12}$$

where $\Delta pq = \bar{p}\Delta q + \bar{q}\Delta p$.

8. WENO-TVD method

In this section, we use the TVD flux (4.6) constructed in section 4 as a building block in the state of the art WENO methods. Here we use the fifth order WENO reconstruction [5].

We consider here the semidiscrete scheme

$$\frac{d}{dt}(u_j(t)) = -\frac{1}{\Delta x}[F_{j+1/2} - F_{j-1/2}] = L_j(u), \tag{8.1}$$

where $F_{j+1/2} = F(u(x_{j+1/2}, t))$ is the numerical flux at $x_{j+1/2}$ and time t.

In the current WENO schemes, the numerical solutions of (8.1) is advanced in time by means the TVD Runge — Kutta method [3]. First, from u_j^n, we reconstruct the point values of the function $u(x, t^n)$ via a suitable nonlinear piecewise polynomial interpolation $P_j(x)$, $x \in I_j$ taking into account the conservation, accuracy and non-oscillatory requirements, for each cell I_j. We use here the WENO reconstruction . As a result, at each cell interface $x_{j+1/2}$ the reconstruction produces two different values of the function $u(x)$, namely the left extrapolated value $u^L_{j+1/2} = P_j(x_{j+1/2})$ and the right extrapolated value $u^R_{j+1/2} = P_{j+1}(x_{j+1/2})$.

The numerical flux function at the cell boundaries $x_{j+1/2}$ is defined as a monotone function of the left and right extrapolated values $u^L_{j+1/2}, u^R_{j+1/2}$

$$F_{j+1/2} = F(u_{j+1/2}, t) = F_{j+1/2}(u^L_{j+1/2}, u^R_{j+1/2}). \tag{8.2}$$

In the next subsection, we will present the WENO reconstruction which supplies the required piecewise polynomial $P_j(x)$.

8.1. WENO reconstruction. For the scalar case, the $(2k-1)$-th order WENO reconstruction of $u_{j+1/2}$ is written as

$$u_{j+1/2} = P_j(x_{j+1/2}) = \sum_{r=0}^{k-1} w_r u_{j+1/2}^{(r)}, \tag{8.3}$$

where $u_{j+1/2}^{(r)}$ is the extrapolated value obtained from cell averages in the rth stencil $S_r = \{x_{j-r}, \ldots, x_{j-r+k-1}\}$, $r = 0, \ldots, k-1$, and w_r are the nonlinear weights [5] written as

$$w_r = \frac{\alpha_r}{\alpha_0 + \alpha_1 + \ldots + \alpha_{k-1}}, \quad r = 0, 1, \ldots, k-1, \tag{8.4}$$

where

$$\alpha_r = \frac{d_r}{(\varepsilon + \beta_r)^2}. \tag{8.5}$$

Here $\varepsilon > 0$ is introduced to prevent the denominator from becoming zero. We take $\varepsilon = 10^{-6}$ in our numerical tests. β_r are so called "smooth indicators" of the stencil S_r. For example, the fifth order WENO reconstruction ($k = 3$) is given as in [8, 5]. The corresponding smoothness indicators are given by

$$\begin{aligned}
\beta_0 &= \frac{13}{12}(u_j - 2u_{j+1} + u_{j+2})^2 + \frac{1}{4}(3u_j - 4u_{j+1} + u_{j+2})^2, \\
\beta_1 &= \frac{13}{12}(u_{j-1} - 2u_j + u_{j+1})^2 + \frac{1}{4}(u_{j-1} - u_{j+1})^2, \\
\beta_2 &= \frac{13}{12}(u_{j-2} - 2u_{j-1} + u_j)^2 + \frac{1}{4}(u_{j-2} - 4u_{j-1} + 3u_j)^2.
\end{aligned} \tag{8.6a}$$

The optimal weights d_r for the left extrapolated value $u_{j+1/2}^L$ at $x_{j+1/2}$ are give by [5]

$$d_0 = \frac{3}{10}, \quad d_1 = \frac{3}{5}, \quad d_2 = \frac{1}{10}, \tag{8.6b}$$

and $u_{j+1/2}^L$ is given by

$$\begin{aligned}
u_{j+1/2}^L = \frac{1}{6} w_0 \left[-u_{j+2} + 5u_{j+1} + 2u_j\right] + \\
\frac{1}{6} w_1 \left[-u_{j-1} + 5u_j + 2u_{j+1}\right] + \frac{1}{6} w_2 \left[2u_{j-2} - 7u_{j-1} + 11u_j\right].
\end{aligned} \tag{8.7}$$

The right value $u_{j+1/2}^R$ is obtained by symmetry.

8.2. Time discretization. Up to now we have only considered spatial discretizations, leaving the time variable continuous. In this section, we consider the issue of time discretization. The time discretization will be implemented by the class of high order TVD Runge — Kutta methods developed in [3].

These Runge — Kutta methods are used to solve the system of initial value problems of ordinary differential equations written as

$$\frac{du}{dt} = L(u), \tag{8.8}$$

where $L(u)$ is the approximation to the derivative $(-F(u)_x)$ in the differential equation (2.1). In [3], schemes of up to third order were found to satisfy the TVD conditions. The optimal third order TVD Runge — Kutta method is given by

$$u^{(1)} = u^n + \Delta t L(u^n), \quad u^{(2)} = \frac{3}{4}u^n + \frac{1}{4}u^{(1)} + \frac{1}{4}\Delta t L(u^{(1)}), \quad u^{n+1} = \frac{1}{3}u^n + \frac{2}{3}u^{(2)} + \frac{2}{3}\Delta t L(u^{(2)}). \tag{8.9}$$

In [3], it has been shown that, even with a very nice second order TVD spatial discretization, if the time discretization is by the non-TVD but the linearly stable Runge — Kutta method, the result may be oscillatory. Thus it would always be safer to use TVD Runge — Kutta methods for hyperbolic problems.

8.3. Description of the method. Titarev and Toro [9] proposed to use the FLIC second order centred TVD flux and the WAF second order upwind TVD flux, instead of first order fluxes as a building block for designing high order schemes. In this section, we propose to use the fourth order TVD flux (4.31) with (4.32) as a building block in the high order WENO schemes with the third order TVD Runge — Kutta method for time stepping.

The derivation of the resulting schemes is straightforward and is summarized in the following algorithm, which applies to the scalar case.

Given the cell averages u_j^n , at time t^n , compute the cell averages at the next time step u_j^{n+1} as follows:

1) obtain $(2k-1)$-th order WENO approximations to the function $u(x)$ at the cell boundaries, denoted by $u^L_{j+1/2}$, $u^R_{j+1/2}$ defined in Eq. (8.7);

2) compute the TVD flux (4.6) with $\Delta_{j+1/2}u = u^R_{j+1/2} - u^L_{j+1/2}$, for all j;

3) form scheme (8.1);

4) using the third order TVD Runge — Kutta method (8.9), compute u_j^{n+1}.

9. Numerical experiments

In this section, we present some numerical experiments to show the performance of our method. For all calculations we use transmissive boundary conditions.

For comparison, we consider the numerical results of the fourth order TVD flux (4.6) and (4.32) with the fifth order WENO reconstruction and compare them to the results obtained by the corresponding original methods that use the second order TVD (FLIC) flux presented by Titarev and Toro [9]. For the time discretization we use, throughout, the third order TVD Runge — Kutta method.

We compare the following schemes:

1) NONTVD: the fully discrete fourth order scheme (4.2) with the flux (4.6) without a limiter;

2) TORO: the Toro scheme with a second order TVD flux with the fifth order WENO reconstruction;

3) YOUTVD: the fully discrete TVD fourth order scheme (4.2) with the flux (4.6) with (4.32);

4) YOUWEN: semidiscrete scheme (8.1) with the fourth order TVD flux (4.6) with (4.32), with the fifth order WENO reconstruction,

5) BG4: the fourth order scheme [1].

Example 9.1. We consider the approximate solution of the linear equation

$$u_t + u_x = 0, \quad -1 < x < 1, \quad t \geqslant 0, \tag{9.1}$$

$$u(x,0) = \sin^4(\pi x), \tag{9.2}$$

with a periodic condition on $[-1,1]$. This test is used to check the convergence rate of the scheme.

Tables 9.1 and 9.2 quote the L^1 errors at a large time $t = 10$. Also the relative L^1 norms of the errors are shown in Table 9.3. We perform several runs with different grid sizes. Here N denotes the total number of spatial cells. We take $\Delta t = 0.8\,\Delta x$. We note that the YOUTVD scheme is even more than fourth order accurate (approximately = 4.3) while the YOUWEN scheme is approximately seventh order accurate. Moreover, the error is much smaller than in the other schemes even on the coarsest meshes. It is noticed from the tables that the NONTVD is more accurate than the YOUTVD. This is due to the use of the limiters that reduce the method to the first order near the discontinuities. Also, we notice that the YOUTVD is about three times slower than the NONTVD scheme. This is due to the use of expensive TVD limiters. However, this difference in the velocity is more than compensated by the improvements in the solution and the removal of oscillations.

Table 9.1.

N	YOUTVD			TORO		
	L^1 error	L^1 order	CPU time	L^1 error	L^1 order	CPU time
80	$6.53E-5$		7.2	$8.82E-4$		29.6
160	$3.22E-6$	4.34	69.27	$2.65E-5$	5.05	289.14
320	$1.63E-7$	4.30	655.22	$2.41E-6$	3.46	2705.54
640	$8.38E-9$	4.28	6173.16	$3.03E-7$	2.99	26453.27

Table 9.2.

N	YOUWEN			NONTVD		
	L^1 error	L^1 order	CPU time	L^1 error	L^1 order	CPU time
80	$2.87E-6$		37.3	$5.30E-5$		2.34
160	$1.56E-8$	7.52	336.50	$2.39E-6$	4.47	23.25
320	$1.42E-10$	6.79	3069.29	$1.053E-7$	4.50	225.06
640	$1.21E-12$	6.87	28098.75	$4.39E-9$	4.59	2175.78

Table 9.3.

N	YOUTVD		TORO		YOUWEN	
	Relative L^1 error	Relative L^1 order	Relative L^1 error	Relative L^1 order	Relative L^1 error	Relative L^1 order
80	$8.35E-5$		$1.18E-3$		$3.41E-6$	
160	$4.23E-6$	4.30	$3.67E-5$	5.00	$1.88E-8$	7.50
320	$2.19E-7$	4.21	$3.38E-6$	3.44	$1.79E-10$	6.71
640	$1.23E-8$	4.22	$4.34E-7$	2.96	$1.62E-12$	6.79

Now we discuss the computational efficiency of the schemes. Tables 9.1 and 9.2 show the CPU times for all schemes. It is noticed from the tables that the YOUTVD and the NONTVD are the fastest schemes because they do not use the WENO reconstructions. The YOUTVD is about three times slower than the NONTVD scheme. This is due to the use of TVD limiters.

Note that the fastest WENO scheme, TORO , is about four times slower than the YOUTVD. This is due to the use of the expensive WENO reconstruction. The YOUWEN is about 26 % slower than the TORO. However, this difference in the velocity is more than compensated by the improvement in the accuracy.

Example 9.2. We now consider equation (9.1) with the initial condition [1]

$$u(x,0) = \begin{cases} [G(x,z-\delta)+G(x,z+\delta)+4G(x,z)]/6, & -0.8 \leqslant x \leqslant -0.6. \\ 1, & -0.4 \leqslant x \leqslant -0.2, \\ 1-|10(x-0.1)|, & 0 \leqslant x \leqslant 0.2, \\ [F(x,a-\delta)+F(x,a+\delta)+4F(x,a)]/6, & 0.4 \leqslant x \leqslant 0.6, \\ 0, & \text{otherwise}, \end{cases} \tag{9.3}$$

with a periodic boundary condition on $[-1,1]$, here $G(x,z) = \exp(-\beta(x-z)^2)$, $F(x,a) = \{\max(1-\alpha^2(x-a)^2,0)\}^{1/2}$. The constants are taken as $a = 0.5$, $z = -0.7$, $\delta = 0.005$, $\alpha = 10$ and $\beta = (\log 2)/36\delta^2$. This initial condition consists of several shapes which are difficult for numerical methods to resolve correctly. Some of these shapes are not smooth and the others are smooth but very sharp. Firstly, we show the effects of the limiters on different profiles of the solutions. Fig. 9.1 shows the numerical results at $t = 20$ obtained by the NONTVD scheme ,without limiters, with a mesh size of 200 cells and $\Delta t = 0.8\,\Delta x$ and Fig. 9.2 shows the same results but by using the YOUTVD with limiters. The exact solution is shown by the solid line and the numerical solution is shown by symbols. It is clear from Fig. 9.1 that the fourth order scheme without limiters generates oscillations around the discontinuities due to the dominating high frequencies dispersion errors. The use of the limiters removes completely these oscillations (Fig. 9.2), producing monotone profiles.

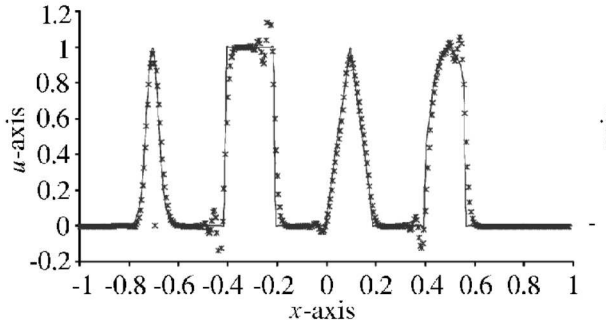

F i g. 9.1. Solution of Eq. (9.1) with (9.3) with the use of the NONTVD scheme at $t = 20$

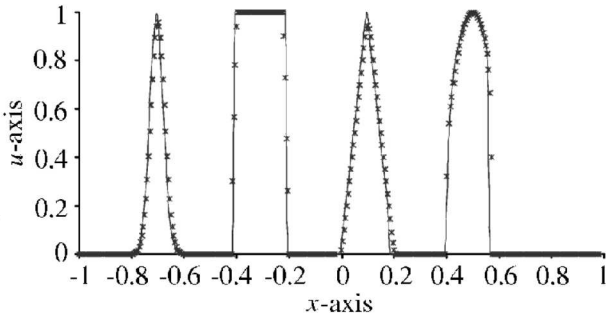

F i g. 9.2. Solution of Eq. (9.1) with (9.3) with the use of the YOUTVD scheme at $t = 20$

Figs. 9.3 and 9.4 show the results obtained by the TORO and YOUWEN schemes respectively. The results in Fig. 9.4 obtained with the YOUWEN are superior to those obtained with all the other methods.

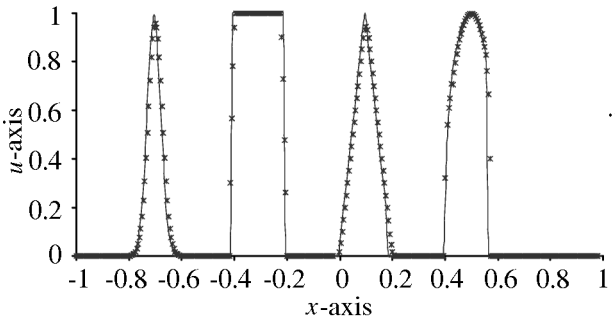

F i g. 9.3. Solution of Eq. (9.1) with (9.3) with the use of the TORO scheme at $t = 20$

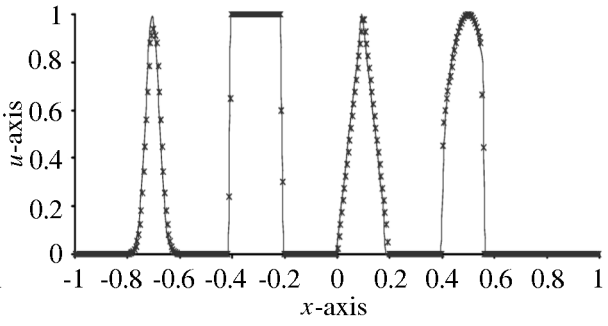

F i g. 9.4. Solution of Eq. (9.1) with (9.3) with YOUWEN scheme at $t = 20$

Example 9.3. In this example we approximate the solution of the Burger equation

$$u_t + [u^2/2]_x = 0 \tag{9.4}$$

with the smooth periodic data

$$u(x,0) = 1 + 0.5 \sin \pi x, \quad -1 \leqslant x \leqslant 1. \tag{9.5}$$

It is well known that the solution of (9.4), (9.5) develops a shock discontinuity at the critical time t = 1.1. Figs. 9.5–9.7 show the results obtained by the YOUTVD, TORO and YOUWEN schemes with mesh size of 80 cells and /delta/t=0.8../delta/x respectively. Note that the numerical solutions in Fig. 9.7 using the YOUWEN scheme is almost indistinguishable from the exact solution.

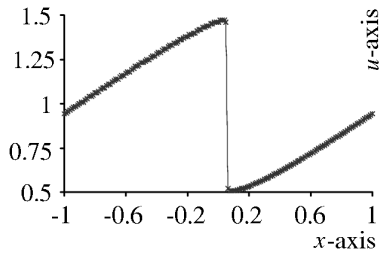

Fig. 9.5. Solution of Eq. (9.4) with (9.5) using the YOUTVD scheme

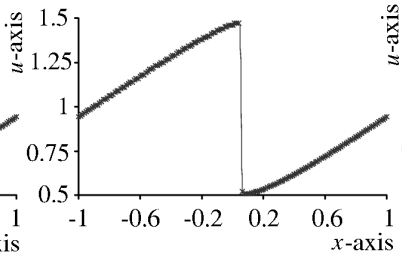

Fig. 9.6. Solution of Eq. (9.4) with (9.5) using the TORO scheme

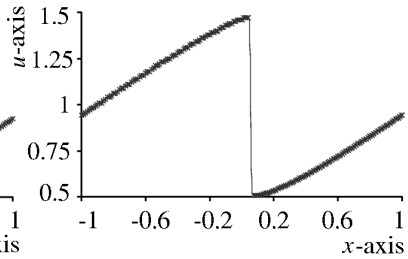

Fig. 9.7. Solution of Eq. (9.4) with (9.5) using the YOUWEN scheme

Table 9.4 shows the CPU times for all the schemes. It is seen from the table that the YOUWEN and TORO schemes are slower than the YOUTVD scheme. This is due to the use of the WENO expensive reconstruction. Considering the improvements in the accuracy compared to the YOUTVD scheme, this additional computational costs is not significant. We note also the YOUWEN scheme is about 25 % slower than the TORO. However, again this difference in the speed is more than compensated by the improvement in the accuracy.

Table 9.4.

Scheme	YOUTVD	TORO	YOUWEN
CPU time	6.32	26.12	32.55

Example 9.4. Here we apply our scheme developed in this paper to Buckley — Leverett's problem, whose flux is non-convex [1]

$$\frac{\partial u}{\partial t} + \frac{\partial f(u)}{\partial x} = 0, \quad -1 \leqslant x \leqslant 1, \quad f(u) = \frac{4u^2}{4u^2 + (1-u)^2} \tag{9.6a}$$

subject to the initial condition

$$u_0(x) = \begin{cases} 1, & x \in [-0.5, 0], \\ 0, & \text{otherwise.} \end{cases} \tag{9.6b}$$

Similarly to Balaguer [1] , we have computed the solution at $t = 0.4$ with the YOUTVD, TORO and YOUWEN schemes. Figs. 9.8–9.10 show the results obtained with $N = 80$ and $\Delta t = 0.8\,\Delta x$. Comparing the results with [1, Fig. 4.4] (with $\Delta t = 0.25\,\Delta x$) we notice that our scheme is more efficient than the BG scheme. It is also noted that the YOUWEN scheme is the best.

Table 9.5 shows the CPU times for all the schemes. Note that the YOUWEN scheme is about 30% slower than the TORO. However, again this difference in the speed is more than compensated by the improvement in the accuracy.

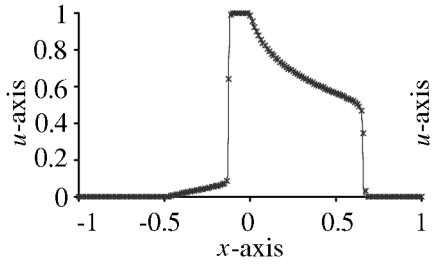

Fig. 9.8. Solution of Eq. (9.6) using the YOUTVD scheme

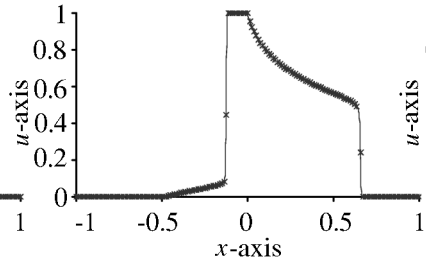

Fig. 9.9. Solution of Eq. (9.6) using the TORO scheme

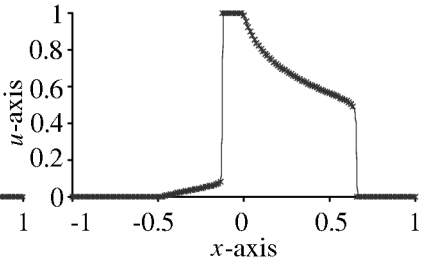

Fig. 9.10. Solution of Eq. (9.6) using the TYOUWEN scheme

Table 9.5.

Scheme	YOUTVD	TORO	YOUWEN
CPU time	4.17	19.5	25.27

Example 9.5. Here we discuss the numerical test results of the solution of RP (7.3) with the initial data of [14]

$$U_L = (0.597,\, 0)^\top, \quad U_R = (0.04166,\, 0)^\top. \tag{9.7}$$

The numerical experiments were performed using the linearized system (7.8)–(7.12) and the YOUTVD, TORO and YOUWEN schemes. Figs. 9.11–9.13 show the exact solution in full lines for the cross-section $S(x,t)$ with the numerical solution shown in symbols. We take $\Delta x = 0.01$, and the Courant number used is 0.8 at $t = 0.228$. Note that the results obtained by the YOUWEN is indistinguishable from the exact solution.

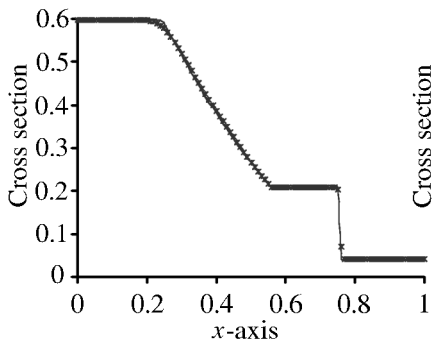

Fig. 9.11. Solution of the shallow water equations using the YOUTVD scheme

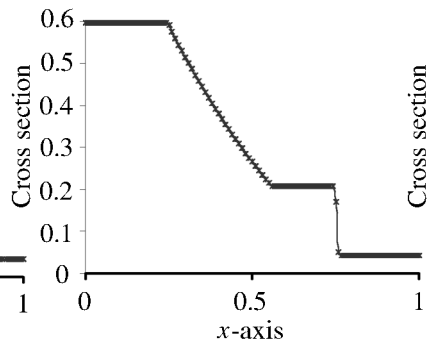

Fig. 9.12. Solution of the shallow water equations using the TORO scheme

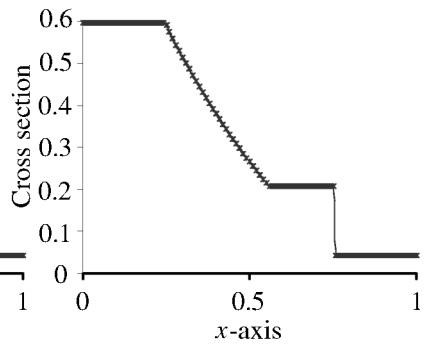

Fig. 9.13. Solution of the shallow water equations using the YOUWEN scheme

Table 9.6 shows the CPU times for all the schemes. We observe that the YOUWENO is about 35 % slower than the TORO scheme. From the numerical results presented here it is seen that this difference is more than compensated by the improvement in the accuracy.

Table 9.6.

Scheme	YOUTVD	TORO	YOUWEN
CPU time	9.76	36.23	48.87

10. Conclusions

Fully discrete and semi-discrete fourth order finite difference schemes for computing solutions to hyperbolic conservation laws have been developed. An oscillations-free version of the schemes has been constructed with the use of flux limiters. We propose to use this fourth order TVD flux as a building block for constructing very high order schemes and have applied the idea to the WENO schemes. The use of this flux within the WENO framework improves the order of accuracy and convergence and betters the resolution of discontinuities. The numerical results suggest that our schemes are superior to the other methods.

References

1. A. Balagur and C. Conde, *Fourth order non-oscillatory upwind and central schemes for hyperbolic conservation laws*, SIAM J. Numer. Anal. **43** (2005), no. 2, pp. 455–473.

2. J. Balbas and E. Tadmor, *Nonoscilatory central schemes for one- and two-dimensional magneto-hydrodynamic equations. II. High-order semidiscrete schemes*, SIAM, J. Sci. Comput. **28** (2006), no. 2, pp. 533–560.

3. F. Bianco, G. Puppo and G. Russo, *High order central schemes for hyperbolic systems of conservation laws*, SIAM J. Sci.Comput. **21** (1999), pp. 294–322.

4. A. Harten, *High resolution scheme for hyperbolic conservation laws*, J. Comut. Phys. **83** (1983), pp. 357–393.

5. G. S. Jiang and C. W. Shu, *Efficient implementation of weighted ENO schemes*, J.Comut. Phys. **126** (1996), pp. 202–228.

6. P. L. Roe, *Numerical algorithms for linear wave equation*, Technical Report 81047, Royal Aircraft Establishments Bedford, U.K., 1981.

7. J. Shi and E. F. Toro, *Fully discrete high order shock capturing numerical schemes*, Int.J. Numer. Methods fluids, **23** (1996), pp. 241–269.

8. C. W. Shu, *Essentially non-oscillatory and weighted ENO for hyperbolic conservation laws*, NASA/ CR no 97-206253, ICASE Report no 97-65 (1997).

9. V. A. Titarev and E. F. Toro, *ENO and WENO schemes based on upwind and centred TVD fluxes*, J. Computers and Fluids, **34** (2005), pp. 705–720.

10. E. F. Toro, *Primtive, conservative and adaptive schemes for hyperbolic conservation laws in numerical methods for wave propagation.* Toro, E. F. and Clarke, J. F.(Editors). Kluwer Academic Publishers, 1998, pp. 323–358.

11. E. F. Toro and S. J. Billett, *Centered TVD schemes for hyperbolic conservation laws*, IMA J. Numerical Analysis. **20** (2000), pp. 47–79.

12. B. Van Leer, *Towards the ultimate conservative difference schemes III. Upstream-centered finite difference schemes for ideal compressible flow*, J. Comput. Phys. **23** (1977), pp. 263–275.

13. B. Van Leer, *On the relation between the upwind differencing schemes of Godunov, Enguist, Osher and Roe*, SIAM J. Sci. Stat. Comput. **5** (1985), pp. 1–20.

14. J. P. Vila, *An analysis of class of second order accurate Godunov type schemes*, SIAM J. Num. Anal. **26** (1989), pp. 830–853.

15. Y. H. Zahran, *A family of TVD second order schemes of nonlinear scalar conservation laws*, J. Comptes rendus de l'Acad. bulgare de sci. **57** (2004), no 2, pp. 9–18.